Prospects for searches for Higgs boson decays to dark photons at the ILC

S. Snyder[1], C. Weber[1], and D. Zhang[2]

[1]*Brookhaven National Laboratory, Upton, NY, 11973*
[2]*Institute of High Energy Physics, Chinese Academy of Sciences, Shijingshan District, Beijing, 100049*

ABSTRACT

An interesting model of dark matter involves a hidden sector decoupled from Standard Model (SM) fields except for some portal interaction. A concrete realization of this is the Hidden Abelian Higgs Model, which gives rise to decays of the SM Higgs boson into a pair of new bosons, called Z_d or dark photons. This note explores prospects for the search for such dark photons at the ILC with $\sqrt{s} = 250\,\mathrm{GeV}$, where the dark photons decay promptly. For the $H \to Z_\mathrm{d}Z_\mathrm{d} \to 4\ell$ ($\ell = e, \mu$) final state, it follows closely recent similar searches at the LHC, while for the $2\ell 2j$ and $4j$ final states a multivariate analysis approach is used. This study has not been approved by the SiD consortium.

1 Introduction

A major open question in particle physics is the nature of the astrophysically-motivated dark matter. An attractive strategy for incorporating dark matter into the Standard Model (SM) is through a hidden sector, decoupled from known SM fields except for some 'portal' interaction [1–11]. A concrete realization of this is the Hidden Abelian Higgs Model
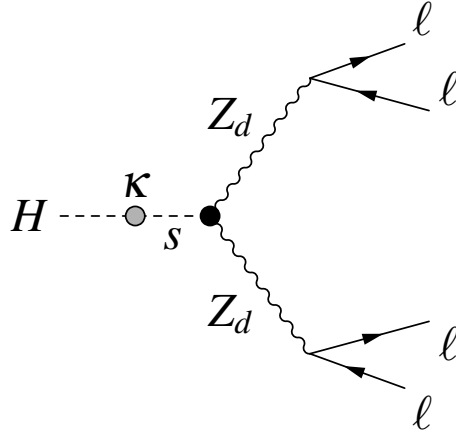
Figure 1: Exotic decay of the Higgs boson into four leptons induced by intermediate dark vector bosons via the Higgs portal, where s is a dark Higgs boson [5]. The $Z_{\rm d}$ gauge boson decays into SM particles through kinetic mixing with the hypercharge field (with branching ratios that are nearly independent of ϵ). The $HZ_{\rm d}Z_{\rm d}$ vertex factor is proportional to κ.

(HAHM) [5–10], in which a new $U(1)_d$ dark gauge field kinetically mixes with the SM $U(1)_Y$ hypercharge gauge field with some strength ϵ [12–14]. This gives rise to a new Higgs-like dark scalar S along with the gauge boson of the new field, $Z_{\rm d}$, or 'dark photon'. The scalar S mixes with the SM Higgs boson with strength κ, allowing decays of the SM Higgs boson into pairs of $Z_{\rm d}$ bosons via mixing with the S scalar. For $\epsilon \ll 1$, the decays of the $Z_{\rm d}$ boson are largely determined by the gauge couplings. Over the range $1\,{\rm GeV} < m_{Z_{\rm d}} < 60\,{\rm GeV}$, the branching fraction of the $Z_{\rm d}$ boson into pairs of electrons or muons could be 10%–15% [5]. These decays would be prompt for $\epsilon \gtrsim 10^{-5}$.

This note explores the prospects for a search for $H \to Z_{\rm d}Z_{\rm d}$ at the ILC with $\sqrt{s} = 250\,{\rm GeV}$, with the $Z_{\rm d}$ bosons decaying promptly to 4ℓ ($\ell \equiv e, \mu$), as illustrated in Fig. 1, as well as $2\ell 2j$ and $4j$. For the 4ℓ final state, it follows closely the analysis of ATLAS at the LHC with $\sqrt{s} = 13\,{\rm TeV}$ and an integrated luminosity of $139\,{\rm fb}^{-1}$ [15]. Other similar searches, including searches for pairs of light bosons decaying into muons, τ-leptons, photons, and/or jets, as well as searches for a single light boson decaying into a pair of muons, using both $\sqrt{s} = 8\,{\rm TeV}$ and $13\,{\rm TeV}$ data, have been performed by ATLAS [16–20], CMS [21–24], and LHCb [25]. Searches for long-lived signatures at ATLAS and CMS are reported in Refs. [26–34], while further searches for a SM Higgs boson decaying into undetected particles are reported in Refs. [35, 36].

The following section describes how the event samples used for these analyses were simulated and reconstructed. This is followed by a description of the $H \to Z_{\rm d}Z_{\rm d} \to 4\ell$, $2\ell 2j$, and $4j$ analyses, including the event selection, a discussion of quarkonia backgrounds, and expected limits. The note ends with a summary and discussion of possible future work.

2 Event simulation and reconstruction

The $ee \to ZH \to ffZ_\mathrm{d}Z_\mathrm{d}$ signal was generated according to the HAHM [5, 6, 9, 10] implementation in MADGRAPH5_aMC@NLO version 2.8.2 [37], with the Higgs boson mass set to $m_H = 125\,\mathrm{GeV}$ and ϵ and κ both set to 10^{-4}. The e^- beam polarization was set to -80% and e^+ to $+30\%$. Leptonically decaying Z_d bosons were forced to decay to either a ee or $\mu\mu$ pair. Final states with τ-leptons were not included. In the similar LHC analysis [15], the change in signal region yield due to the omission of these decays was below 1% and thus neglected. Decays of Z_d bosons to jets were allowed to be inclusive. Other Higgs boson production mechanisms, which are much smaller at the ILC with $\sqrt{s} = 250\,\mathrm{GeV}$, were also omitted. Showering was performed via MADGRAPH5_aMC@NLO's built-in interface to PYTHIA 8.244 [38]. Events in the 4ℓ final state were generated at $m_{Z_\mathrm{d}} = 1\,\mathrm{GeV}$, every $2\,\mathrm{GeV}$ in the range $2\,\mathrm{GeV} \leq m_{Z_\mathrm{d}} \leq 12\,\mathrm{GeV}$, and every $5\,\mathrm{GeV}$ in the range $15\,\mathrm{GeV} \leq m_{Z_\mathrm{d}} \leq 60\,\mathrm{GeV}$. Signal samples with $2\ell2j$ and $4j$ final states were produced at $mZd = 20\,\mathrm{GeV}$, $40\,\mathrm{GeV}$, and $60\,\mathrm{GeV}$. Each signal sample was generated with 20,000 events per m_{Z_d} value and per final state.

The $ee \to X + H \to X + 4\ell$ background was generated using WHIZARD 2.8.5 [39, 40] along with its internal version of PYTHIA 6.4 [41], with parameters set corresponding to the OPAL tune provided in [42]. The e^- beam polarization was set to -80% and e^+ to $+30\%$, and the provided `ilc250` CIRCE2 parameterization was used. The Higgs boson was forced to decay into either a $4e$, $2e2\mu$, or 4μ final state. For this background, 20,000 events were generated.

The non-resonant $ee \to 4e, 2e2\mu, 4\mu$ background was also generated with WHIZARD, using the same settings as described previously. To remove divergences, the final state leptons were restricted to be within $20° < \theta < 160°$; further, each pair of final state leptons had to have an invariant mass greater than $1\,\mathrm{GeV}$. For this background, 250,000 events were generated.

The generated events were processed through the full iLCSoft simulation and reconstruction chain [43] using the `o2_V03` version of the SiD [44] geometry. The electrons and muons used in the analysis were identified by `IsolatedLeptonTaggingProcessor` [45]. This, however, relies on a cone-based isolation algorithm that rejects leptons from $Z_\mathrm{d} \to \ell\ell$ decay if $m_{Z_\mathrm{d}} \lesssim 4\,\mathrm{GeV}$. In order extend the analysis to smaller values of m_{Z_d}, the isolation algorithm is modified. When summing the particle flow objects inside an isolation cone around an electron or muon candidate, the highest-energy same-flavor opposite-sign lepton candidate is ignored. This recovers efficiency for $Z_\mathrm{d} \to \ell\ell$ at low m_{Z_d} with no significant increase in background for this analysis (as estimated from a $b\bar{b}$ sample generated with WHIZARD).

The $2\ell2j$ and $4j$ final states rely on inclusive $ee \to ZH$ and $ee \to ZZ$ samples from the SiD collaboration [46]. These were generated using WHIZARD 2.6.4 using nominal ILC Technical Design Report polarization fractions of 80% polarized electrons and 30% polarized positrons. However the study is limited to samples with -80% and e^+ to $+30\%$ polarization to match electron beam polarization of the signal samples, and has not been approved by the SiD consortium.

3

3 $H \to Z_{\mathbf{d}} Z_{\mathbf{d}} \to 4\ell$ event selection

The event selection closely follows that of the ATLAS $H \to Z_{\mathrm{d}} Z_{\mathrm{d}} \to 4\ell$ analysis [15], with a few modifications for the ILC environment, such as removing detector-specific particle-identification requirements and changing requirements on p_{T} and η to E and θ. Although each signal event contains a Z boson decay in addition to the Higgs boson decay, no explicit requirements are made for the Z boson decay. Two sets of selections are used. The first, called the high-mass (HM) selection is designed for $15\,\mathrm{GeV} < m_{Z_{\mathrm{d}}} < 60\,\mathrm{GeV}$, and the second, low-mass (LM), selection is designed for $1\,\mathrm{GeV} < m_{Z_{\mathrm{d}}} < 15\,\mathrm{GeV}$. In this latter region, the angular separation between the two leptons from $Z_{\mathrm{d}} \to \ell\ell$ decay becomes small. For the ATLAS analysis [15], the LM analysis used only the 4μ final state, due to a decreased efficiency for identifying closely-spaced electrons. Simulated ILC events do not show such a drop in efficiency, so here all final states are used for the LM analysis.

Electrons and muons must satisfy $E > 7\,\mathrm{GeV}$ and $0.35 < \theta < \pi - 0.35$. Such leptons are formed into quadruplets consisting of two same-flavor opposite-sign (SFOS) lepton pairs, giving $4e$, $2e2\mu$, and 4μ final states. If there are more than two such pairs, multiple quadruplets are formed from all possible SFOS combinations. The invariant masses of the two pairs are denoted by m_{12} and m_{34}, with m_{12} taken to be the one closest to the mass of the Z boson: $|m_{12} < m_Z| < |m_{34} - m_Z|$.

If all four leptons in a quadruplet have the same flavor, then one can also define alternate pairings. The invariant mass m_{14} is defined from the positively charged lepton of the m_{12} pair and the negatively charged lepton of the m_{34} pair. The other alternative pairing m_{23} is defined similarly.

For all quadruplets, the three highest-energy leptons must satisfy $E_1 > 20\,\mathrm{GeV}$, $E_2 > 15\,\mathrm{GeV}$, and $E_3 > 10\,\mathrm{GeV}$. For the HM analysis only, the angular separation between all same-flavor leptons must satisfy $\Delta R(\ell, \ell') > 0.1$ and for different-flavor leptons $\Delta R(\ell, \ell') > 0.2$, where $(\Delta R)^2 = (\Delta\eta)^2 + (\Delta\phi)^2$ and η is the pseudorapidity[*]. Events are required to have at least one such quadruplet. If there is more than one, the quadruplet with the smallest $\Delta m_{\ell\ell} = |m_{12} - m_{34}|$ is used.

For the HM event selection, the invariant mass of the four leptons must be consistent with that of the SM Higgs boson: $115\,\mathrm{GeV} < m_{4\ell} < 130\,\mathrm{GeV}$. The quadruplet must also not be consistent with the decay of Z bosons (Z-veto): $10\,\mathrm{GeV} < m_{12,34} < 64\,\mathrm{GeV}$. For the $4e$ and 4μ channels, it is possible that the leptons are mispaired, so for these channels there is also a requirement on the alternative lepton pairings: $5\,\mathrm{GeV} < m_{14,23} < 75\,\mathrm{GeV}$. Events with lepton pairs consistent with J/ψ or Υ decay are also rejected. Events are rejected if any of $m_{12,34,14,23}$ are in the ranges $(m_{J/\psi} - 0.25\,\mathrm{GeV})$ to $(m_{\psi(2S)} + 0.30\,\mathrm{GeV})$ or $(m_{\Upsilon(2S)} - 0.70\,\mathrm{GeV})$ to $(m_{\Upsilon(3S)} + 0.75\,\mathrm{GeV})$, where the quarkonia masses are taken to be $m_{J/\psi} = 3.096\,\mathrm{GeV}$, $m_{\psi(2S)} = 3.686\,\mathrm{GeV}$, $m_{\Upsilon(1S)} = 9.461\,\mathrm{GeV}$, and $m_{\Upsilon(3S)} = 10.355\,\mathrm{GeV}$ [47]. Finally, a requirement $m_{34}/m_{12} > 0.85$ ensures that the two pairs have similar invariant masses.

---

[*]Although an analysis in an e^-e^+ environment would more naturally use θ than η, the use of ΔR is retained here for consistency with the ATLAS analysis.

4

Table 1: Summary of event selection requirements for the HM and LM analyses.

		High-mass (HM) analysis $H \to Z_{\mathrm{d}}Z_{\mathrm{d}} \to 4\ell$ ($\ell = e, \mu$)	Low-mass (LM) analysis $H \to Z_{\mathrm{d}}Z_{\mathrm{d}} \to 4\ell$ ($\ell = e, \mu$)
Mass range		$15\,\mathrm{GeV} < m_X < 60\,\mathrm{GeV}$	$1\,\mathrm{GeV} < m_X < 15\,\mathrm{GeV}$
Leptons		Four isolated electrons or muons with $E > 7\,\mathrm{GeV}$ and $0.35 < \theta < \pi - 0.35$	
Quadruplet selection		$e^+e^-e^+e^-$, $e^+e^-\mu^+\mu^-$, or $\mu^+\mu^-\mu^+\mu^-$; Three leading-E leptons satisfying $E > 20\,\mathrm{GeV}$, $15\,\mathrm{GeV}$, $10\,\mathrm{GeV}$ Define pairs m_{12} and m_{34} such that $|m_{12} - m_Z| < |m_{34} - m_Z|$	
		$\Delta R(\ell, \ell') > 0.10\,(0.20)$ for same-flavor (different-flavor) ℓ, ℓ'	—
Quadruplet ranking		Select quadruplet with smallest $\Delta m_{\ell\ell} = |m_{12} - m_{34}|$	
Event selection	$m_{4\ell}$	$115\,\mathrm{GeV} < m_{4\ell} < 130\,\mathrm{GeV}$	$120\,\mathrm{GeV} < m_{4\ell} < 130\,\mathrm{GeV}$
	Z-veto	$10\,\mathrm{GeV} < m_{12,34} < 64\,\mathrm{GeV}$ For $4e$ and 4μ channels: $5\,\mathrm{GeV} < m_{14,23} < 75\,\mathrm{GeV}$	—
	Heavy-flavor veto	Reject event if $m_{12,34,14,23}$ in: $(m_{J/\psi} - 0.25\,\mathrm{GeV})$ to $(m_{\psi(2S)} + 0.30\,\mathrm{GeV})$, or $(m_{\Upsilon(1S)} - 0.70\,\mathrm{GeV})$ to $(m_{\Upsilon(3S)} + 0.75\,\mathrm{GeV})$	Reject event if $m_{14,23}$ in: $(m_{J/\psi} - 0.25\,\mathrm{GeV})$ to $(m_{\psi(2S)} + 0.30\,\mathrm{GeV})$, or $(m_{\Upsilon(1S)} - 0.70\,\mathrm{GeV})$ to $(m_{\Upsilon(3S)} + 0.75\,\mathrm{GeV})$
	Signal region	$m_{34}/m_{12} > 0.85$	$0.8\,\mathrm{GeV} < m_{12,34} < 20\,\mathrm{GeV}$ $m_{34}/m_{12} > 0.85$

For the LM event selection, the pair invariant masses are required to be in the range $0.8\,\mathrm{GeV} < m_{12,34} < 20\,\mathrm{GeV}$. The requirement on the overall invariant mass is tightened to $120\,\mathrm{GeV} < m_{4\ell} < 130\,\mathrm{GeV}$ due to smaller radiative tails in this regime. The Z-veto requirement is not applied, and and only the alternate lepton pairings are used for the quarkonia vetoes (see Section 4). The final requirement $m_{34}/m_{12} > 0.85$ is the same as for the HM analysis.

Both event selections are summarized in Table 1.

The main backgrounds are from SM $H \to ZZ^* \to 4\ell$ decay and also from nonresonant 4ℓ production, with the latter source dominating. These are estimated using the simulated samples described in Section 2. Backgrounds in which jets are misidentified as leptons are assumed to be negligible. Estimated backgrounds for a data sample of $2000\,\mathrm{fb}^{-1}$ are shown in Table 2.

Table 2: Estimated backgrounds for the $H \to Z_{\mathrm{d}} Z_{\mathrm{d}} \to 4\ell$ analyses for a data sample of $2000\,\mathrm{fb}^{-1}$. No simulated events for the non-resonant background pass the LM selection, so a limit is given based on the background represented by one simulated event.

HM selection	$4e$	$2e2\mu$	4μ	All
$H \to ZZ^* \to 4\ell$	0.37 ± 0.04	0.39 ± 0.04	0.46 ± 0.04	1.22 ± 0.07
Non-resonant	3.05 ± 1.15	2.62 ± 1.07	0.44 ± 0.44	6.10 ± 1.63
Total	3.42 ± 1.15	3.00 ± 1.07	0.90 ± 0.44	7.32 ± 1.63

LM selection	$4e$	$2e2\mu$	4μ	All
$H \to ZZ^* \to 4\ell$	0.04 ± 0.01	< 0.01	0.03 ± 0.01	0.07 ± 0.02
Non-resonant	< 0.44	< 0.44	< 0.44	< 0.44
Total	< 0.47	< 0.44	< 0.47	< 0.51

4   Quarkonia backgrounds to $H \to Z_{\mathrm{d}} Z_{\mathrm{d}} \to 4\ell$ final states

The ATLAS $H \to Z_{\mathrm{d}} Z_{\mathrm{d}} \to 4\ell$ analysis [15] has no sensitivity in the regions $2\,\mathrm{GeV} < m_{Z_{\mathrm{d}}} < 4.4\,\mathrm{GeV}$ and $8\,\mathrm{GeV} < m_{Z_{\mathrm{d}}} < 12\,\mathrm{GeV}$ due to the presence of large backgrounds from quarkonia production. However, at the ILC, hadronic backgrounds such as this will be much smaller, and the excellent lepton momentum resolution of the ILC detectors may reduce the size of the $m_{Z_{\mathrm{d}}}$ ranges affected by these backgrounds. Unfortunately, there is no reliable, general-purpose simulation of quarkonia production at the ILC. But one can still estimate these backgrounds, as described below.

First, consider direct, non-resonant production of J/ψ and Υ pairs. These processes were estimated using HELAC-ONIA version 2.0.1 [48, 49]. This can calculate processes such as $e^- e^+ \to J/\psi J/\psi$ and $e^- e^+ \to J/\psi J/\psi + q\bar{q}$, and similarly for Υ. The quarkonia can be produced as either color singlets or color octets. For the purpose of this study, excited quarkonia states are not considered. The initial beams are set to $e^- e^+$ with beam energies of $125\,\mathrm{GeV}$ each, with initial-state radiation disabled. (HELAC-ONIA does not implement beam polarization effects, and enabling initial-state radiation caused the subsequent showering step to fail.) For the processes with the largest cross sections, generated events were then showered and hadronized with PYTHIA 8.244, with the quarkonia forced to decay to either $e^- e^+$ or $\mu^- \mu^+$. The quarkonia decay branching ratios were taken to be $\mathrm{BR}(J/\psi \to \ell\ell) = 0.119$ and $\mathrm{BR}(\Upsilon \to \ell\ell) = 0.049$ [47]. Events were then passed through the detector simulation and analysis, yielding estimates of these quarkonia backgrounds after the LM selection, shown in Table 3. These estimates are all much smaller than other backgrounds for this selection.

Another possibility is the decay of a Z boson into a quarkonia pair, or two Z bosons decaying to the same quarkonium state. Backgrounds from these processes were estimated using current experimental limits/measurements for such decays [47]:

Table 3: Quarkonia production processes calculated with HELAC-ONIA. The ^{1} and ^{8} superscripts denote color-singlet and color-octet states, respectively. For the processes with larger cross sections, the number of expected events passing the LM selection for a data sample of $2000\,\mathrm{fb}^{-1}$ is shown. This is shown as a limit for cases where no simulated events pass the selection.

Process	Cross section (ab)	Expected background
$J/\psi^{\mathbf{1}} J/\psi^{\mathbf{1}}$	8.3	$<5.7 \times 10^{-6}$
$J/\psi^{\mathbf{8}} J/\psi^{\mathbf{8}}$	2.9×10^{-6}	
$J/\psi^{\mathbf{1}} J/\psi^{\mathbf{1}} + d\bar{d}$	0.0033	
$J/\psi^{\mathbf{8}} J/\psi^{\mathbf{8}} + d\bar{d}$	11	<0.0018
$J/\psi^{\mathbf{1}} J/\psi^{\mathbf{1}} + u\bar{u}$	0.0017	
$J/\psi^{\mathbf{8}} J/\psi^{\mathbf{8}} + u\bar{u}$	45	<0.0034
$J/\psi^{\mathbf{1}} J/\psi^{\mathbf{1}} + s\bar{s}$	0.0033	
$J/\psi^{\mathbf{8}} J/\psi^{\mathbf{8}} + s\bar{s}$	11	<0.0018
$J/\psi^{\mathbf{1}} J/\psi^{\mathbf{1}} + c\bar{c}$	0.057	
$J/\psi^{\mathbf{8}} J/\psi^{\mathbf{8}} + c\bar{c}$	41	6.3×10^{-4}
$J/\psi^{\mathbf{1}} J/\psi^{\mathbf{1}} + b\bar{b}$	0.0022	
$J/\psi^{\mathbf{8}} J/\psi^{\mathbf{8}} + b\bar{b}$	8.3	1.0×10^{-4}
$J/\psi^{\mathbf{1}} J/\psi^{\mathbf{1}} + gg$	0.012	
$J/\psi^{\mathbf{8}} J/\psi^{\mathbf{8}} + gg$	1.6	a
$J/\psi^{\mathbf{8}} J/\psi^{\mathbf{8}} + g$	0.060	1.1×10^{-6}
$\Upsilon^{\mathbf{1}} \Upsilon^{\mathbf{1}}$	0.18	$<1.3 \times 10^{-7}$
$\Upsilon^{\mathbf{8}} \Upsilon^{\mathbf{8}}$	6.5×10^{-11}	
$\Upsilon^{\mathbf{1}} \Upsilon^{\mathbf{1}} + d\bar{d}$	8.1×10^{-4}	
$\Upsilon^{\mathbf{8}} \Upsilon^{\mathbf{8}} + d\bar{d}$	1.0×10^{-5}	
$\Upsilon^{\mathbf{1}} \Upsilon^{\mathbf{1}} + u\bar{u}$	0.0034	
$\Upsilon^{\mathbf{8}} \Upsilon^{\mathbf{8}} + u\bar{u}$	4.0×10^{-5}	
$\Upsilon^{\mathbf{1}} \Upsilon^{\mathbf{1}} + s\bar{s}$	8.1×10^{-4}	
$\Upsilon^{\mathbf{8}} \Upsilon^{\mathbf{8}} + s\bar{s}$	1.0×10^{-5}	
$\Upsilon^{\mathbf{1}} \Upsilon^{\mathbf{1}} + c\bar{c}$	0.0031	
$\Upsilon^{\mathbf{8}} \Upsilon^{\mathbf{8}} + c\bar{c}$	3.9×10^{-5}	
$\Upsilon^{\mathbf{1}} \Upsilon^{\mathbf{1}} + b\bar{b}$	0.0022	
$\Upsilon^{\mathbf{8}} \Upsilon^{\mathbf{8}} + b\bar{b}$	8.4×10^{-6}	
$\Upsilon^{\mathbf{1}} \Upsilon^{\mathbf{1}} + gg$	4.7×10^{-5}	
$\Upsilon^{\mathbf{8}} \Upsilon^{\mathbf{8}} + gg$	8.0×10^{-5}	
$\Upsilon^{\mathbf{1}} \Upsilon^{\mathbf{1}} + g$	2.9×10^{-7}	

^{a}HELAC-ONIA failed to generate events for this process.

$$\begin{array}{ll} \text{BR}(Z \to J/\psi + X) & 5.1 \times 10^{-3} \\ \text{BR}(Z \to J/\psi J/\psi) & <2.2 \times 10^{-6} \\ \text{BR}(Z \to \Upsilon + X) & 1.0 \times 10^{-4} \\ \text{BR}(Z \to \Upsilon\Upsilon) & <1.5 \times 10^{-6} \end{array}$$

WHIZARD was used to generate a sample of $e^-e^+ \to f\bar{f}Z$, where f is any fermion, configured as described in Section 2, except that the PYTHIA showering was set to force the Z boson to decay as either $Z \to J/\psi J/\psi \to 4\ell$ or $Z \to \Upsilon\Upsilon \to 4\ell$. Events were then passed through the detector simulation and LM selection. The total cross section calculated by WHIZARD for $f\bar{f}Z$ was 7.1×10^3 fb. Taking into account the branching ratios above and the efficiency of the LM selection, the expected background for a $2000\,\text{fb}^{-1}$ data sample is $< 2.2 \times 10^{-5}$ for $Z \to J/\psi J/\psi$ and 1.2×10^{-5} for $Z \to \Upsilon\Upsilon$.

Similarly, WHIZARD was also used to generate a sample of $e^-e^+ \to ZZ$, where here each Z boson was forced to decay as either $Z \to J/\psi c\bar{c}$ or $Z \to \Upsilon b\bar{b}$. The total WHIZARD cross section for this process was 1.8×10^3 fb. Again, taking into account branching ratios and efficiencies, the expected background for a $2000\,\text{fb}^{-1}$ data sample is 0.0029 for $ZZ \to J/\psi J/\psi + c\bar{c}c\bar{c}$ and 4.3×10^{-7} for $ZZ \to \Upsilon\Upsilon + b\bar{b}b\bar{b}$.

A final possibility is $H \to J/\psi J/\psi$ or $H \to \Upsilon\Upsilon$. Such a background would be particularly concerning since it could not be removed by the requirement that the overall invariant mass be consistent with that of the SM Higgs boson. However, calculations give $BR(H \to J/\psi J/\psi) = 5.9 \times 10^{-10}$ and $BR(H \to \Upsilon\Upsilon) = 4.3 \times 10^{-10}$ [50, 51], which are much smaller than the $H \to Z_\text{d}Z_\text{d}$ branching ratio to which the LM analysis is sensitive.

Although this does not exhaust all possibilities for quarkonia background processes, it should be a representative sample. All processes examined result in backgrounds that are much smaller than the other (already-small) backgrounds to the LM selection. Therefore, quarkonia production is unlikely to be a significant background to this analysis. However, evaluating this with more confidence would likely require improved codes for calculating quarkonia processes.

Further, the invariant mass distributions of dilepton decays of quarkonia are shown in Fig. 2. These events were generated by HELAC-ONIA +PYTHIA and processed with the full detector simulation. (HELAC-ONIA sets the quarkonia masses to be exactly the sum of the masses of the constituent quarks, so the positions of the peaks are shifted from the true quarkonia masses.) These peaks are very narrow, especially for the $\mu^-\mu^+$ decays. Therefore, even if quarkonia backgrounds were to be significant, they could be effectively suppressed by rejecting a much smaller range in m_{Z_d} than was done in the ATLAS analysis.

5 $H \to Z_\mathbf{d}Z_\mathbf{d} \to 4\ell$ expected limits

Expected limits are set based on the distribution of the average of the invariant masses of the two lepton pairs in a quadruplet, $\langle m_{\ell\ell} \rangle = \frac{1}{2}(m_{12} + m_{34})$. The likelihood function
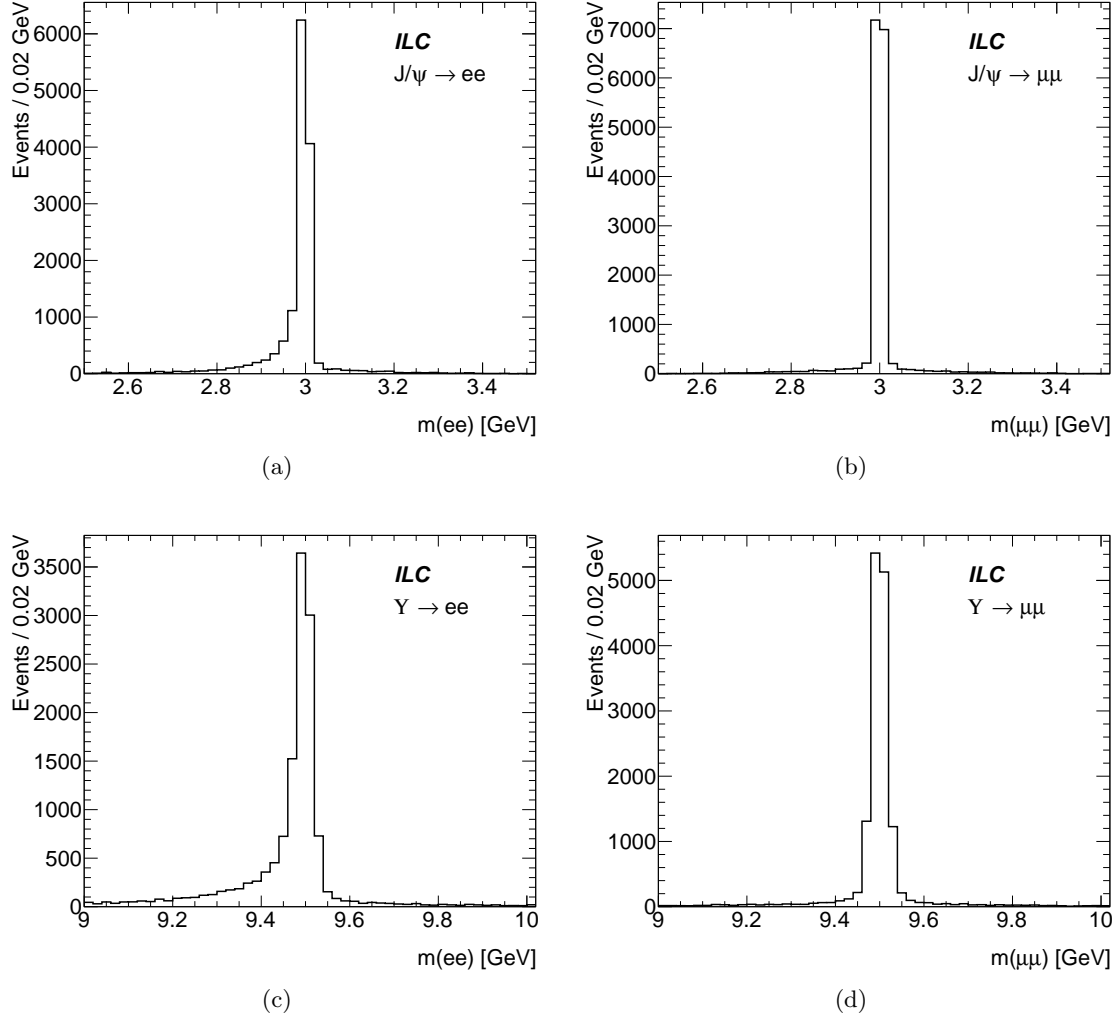
Figure 2: Invariant mass distributions for quarkonia decays to lepton pairs as generated by HELAC-ONIA +PYTHIA: (a) $J/\psi \to e^-e^+$; (b) $J/\psi \to \mu^-\mu^+$; (c) $\Upsilon \to e^-e^+$; (d) $\Upsilon \to \mu^-\mu^+$. Note that HELAC-ONIA sets the quarkonia masses to be exactly the sum of the constituent quark masses; hence, the peaks are shifted from the true quarkonia masses.
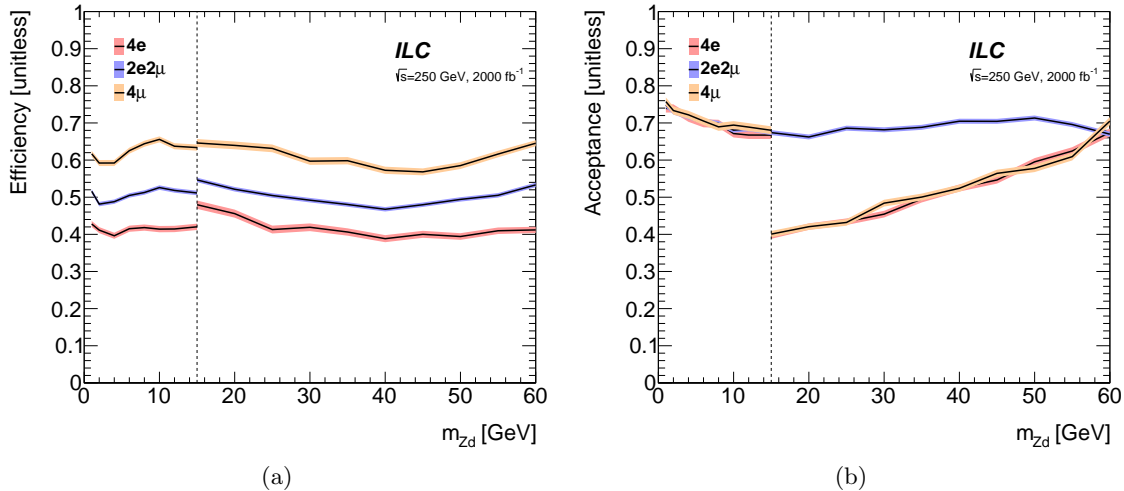
Figure 3: (a) Model-independent per-channel efficiencies for the fiducial volumes described in Table 4. (b) Model-dependent per-channel acceptances for the $H \to Z_\mathrm{d} Z_\mathrm{d} \to 4\ell$ process. The discontinuities at $m_{Z_\mathrm{d}} = 15\,\mathrm{GeV}$ are due to the change from the LM to HM selection.

describing the data for a channel j consists of a Poisson factor for each histogram bin i:

$$\mathcal{L}(N) = \prod_i \mathrm{Pois}\left(N_{ij}; \mu S_{ij}(m_{Z_\mathrm{d}}) + B_{ij}\right), \tag{1}$$

where S and B are the predicted numbers of signal and background events for each bin and channel and μ is the signal strength. For this study, systematic uncertainties are assumed to be negligible. The signal shape as a function of m_{Z_d} is found by fitting a Gaussian to the simulated signal at each generated mass point and then interpolating in the fit mean and width as a function of m_{Z_d}. Background histograms are smoothed using the `RooKeysPdf` class of ROOFIT [52, 53], except that if there are less then ten simulated events surviving in a channel, the background is taken to be flat with respect to m_{Z_d}.

Following [15], a set of generator-level fiducial requirements, described in Table 4, are used to factorize the event selection into a largely model-independent 'efficiency' and a model-dependent 'acceptance'. For the purpose of these selections, the four-momenta of photons close to a lepton ($\Delta R < 0.1$) are added to that of the lepton. This accounts for the effects of quasi-collinear electromagnetic radiation from the leptons [54]. The efficiency for a channel is defined as the fraction of events passing the generator-level fiducial selection that also passes the full event selection, while the acceptance is defined as the fraction of generator-level events that pass the fiducial selection. The efficiency and acceptance for the analyses described here are shown in Fig. 3. For the HM selection, the acceptance falls for low m_{Z_d} for the 4e and 4μ channels due to the alternate pair requirement of the Z-veto. (Similar behavior was seen in the ATLAS analysis [15].)

The efficiencies are used to compute expected 95% CL upper limits on the cross sections within the fiducial region, using the $\mathrm{CL_s}$ frequentist formalism [55] with the profile-

10

Table 4: Summary of the fiducial phase-space definitions for the HM and LM analyses. Objects are considered at generator-level, with photons nearby leptons summed with those leptons.

	High-mass (HM) analysis $H \to Z_\mathrm{d} Z_\mathrm{d} \to 4\ell$ ($\ell = e, \mu$)	Low-mass (LM) analysis $H \to Z_\mathrm{d} Z_\mathrm{d} \to 4\ell$ ($\ell = e, \mu$)
Mass range	$15\,\mathrm{GeV} < m_X < 60\,\mathrm{GeV}$	$1\,\mathrm{GeV} < m_X < 15\,\mathrm{GeV}$
Leptons	$E > 7\,\mathrm{GeV}$ and $0.35 < \theta < \pi - 0.35$	
Quadruplet	Three leading-E leptons satisfying $E > 20\,\mathrm{GeV}, 15\,\mathrm{GeV}, 10\,\mathrm{GeV}$	
	$\Delta R(\ell, \ell') > 0.10\,(0.20)$ for same-flavor (different-flavor) ℓ, ℓ'	—
	$m_{34}/m_{12} > 0.85$	
	$10\,\mathrm{GeV} < m_{12,34} < 64\,\mathrm{GeV}$ For $4e$ and 4μ channels: $5\,\mathrm{GeV} < m_{14,23} < 75\,\mathrm{GeV}$	$0.8\,\mathrm{GeV} < m_{12,34} < 20\,\mathrm{GeV}$
	Reject event if $m_{12,34,14,23}$ in: $(m_{J/\psi} - 0.25\,\mathrm{GeV})$ to $(m_{\psi(2S)} + 0.30\,\mathrm{GeV})$, or $(m_{\Upsilon(1S)} - 0.70\,\mathrm{GeV})$ to $(m_{\Upsilon(3S)} + 0.75\,\mathrm{GeV})$	Reject event if $m_{14,23}$ in: $(m_{J/\psi} - 0.25\,\mathrm{GeV})$ to $(m_{\psi(2S)} + 0.30\,\mathrm{GeV})$, or $(m_{\Upsilon(1S)} - 0.70\,\mathrm{GeV})$ to $(m_{\Upsilon(3S)} + 0.75\,\mathrm{GeV})$

likelihood-ratio test statistic [56], and are shown in Fig. 4, assuming a total integrated luminosity of $2000\,\mathrm{fb}^{-1}$. Incorporating the acceptance and combining the channels, this can be converted into an upper limit on the product of the total cross section and the decay branching ratio for the model considered, $\sigma(e^+ e^- \to H + X \to Z_\mathrm{d} Z_\mathrm{d} + X \to 4\ell + X)$, shown in Fig. 5a. Using the model-dependent branching ratio $\mathrm{BR}(Z_\mathrm{d} \to 2\ell)$, this can be converted into an limit on $\mathrm{BR}(H \to Z_\mathrm{d} Z_\mathrm{d})$, shown in Fig. 5b.

Compared to limits from the similar ATLAS analysis with $139\,\mathrm{fb}^{-1}$ of data and $\sqrt{s} = 13\,\mathrm{TeV}$, the expected branching ratio limits here are a factor of 5–10 higher. This is not unexpected: since the background is quite small, even at the LHC, the sensitivity is driven mainly by the total number of Higgs bosons produced, which was about ten times larger at the LHC than would be expected in $2000\,\mathrm{fb}^{-1}$ of ILC data at $\sqrt{s} = 250\,\mathrm{GeV}$. The exception is in the mass ranges $2\,\mathrm{GeV} < m_{Z_\mathrm{d}} < 4.4\,\mathrm{GeV}$ and $8\,\mathrm{GeV} < m_{Z_\mathrm{d}} < 12\,\mathrm{GeV}$, where the ATLAS analysis has no sensitivity due to quarkonia backgrounds.

6 $H \to Z_\mathbf{d} Z_\mathbf{d} \to 2\ell 2j$, $4j$ event selection

The event selection for the $2\ell 2j$ and $4j$ final states proceeds in two steps, beginning with a cut-based preselection followed by a selection based on boosted decision trees (BDT).

The $2\ell 2j$ final state requires at least one pair of opposite-sign electrons or muons along with four jets formed from particle flow objects (PFO) not associated with isolated leptons
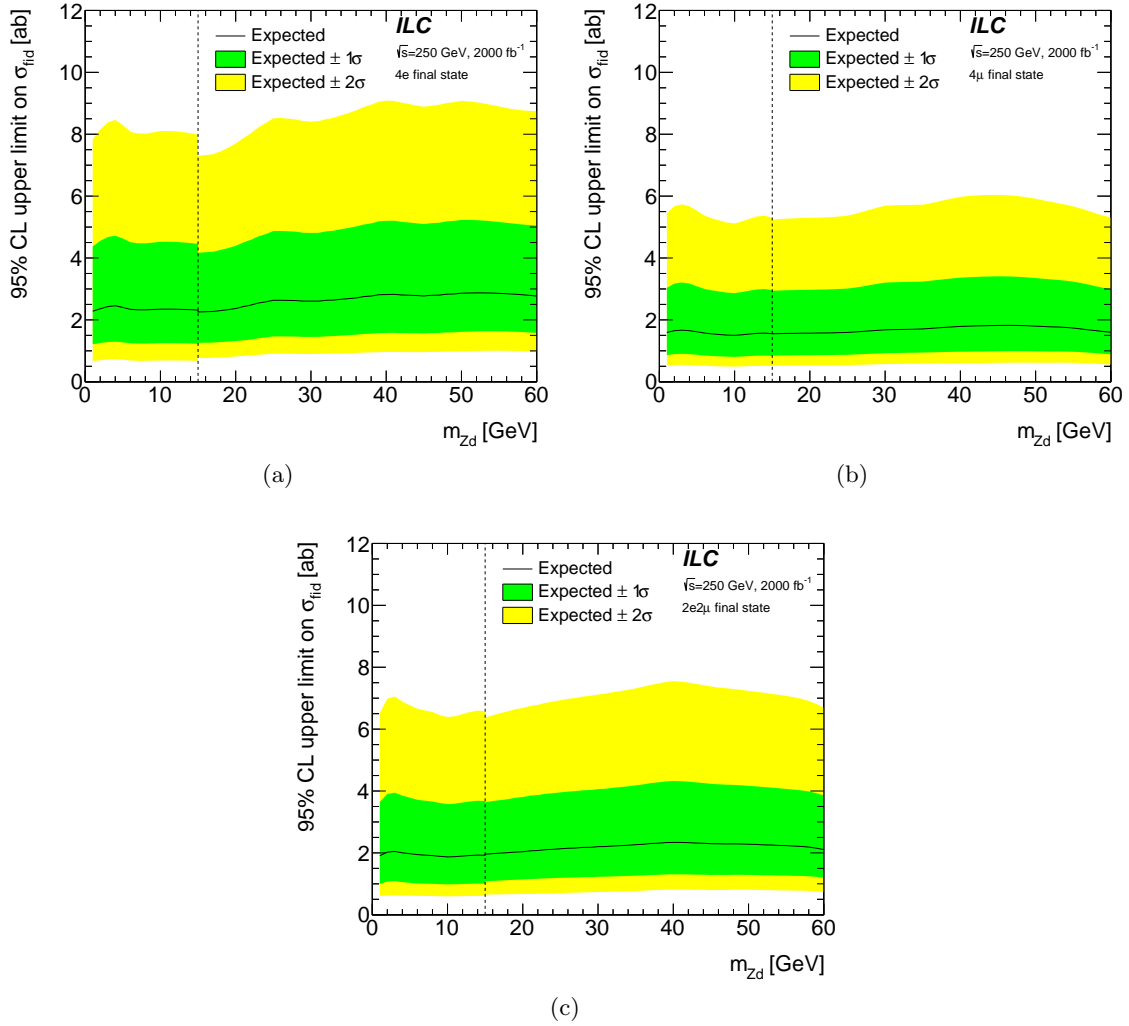
Figure 4: Per-channel expected upper limits at 95% CL on the fiducial cross sections for the $H \to Z_\mathrm{d} Z_\mathrm{d} \to 4\ell$ process, for the (a) $4e$, (b) 4μ, and (c) $2e2\mu$ final states. The discontinuities at $m_{Z_\mathrm{d}} = 15\,\mathrm{GeV}$ are due to the change from the LM to HM selection.
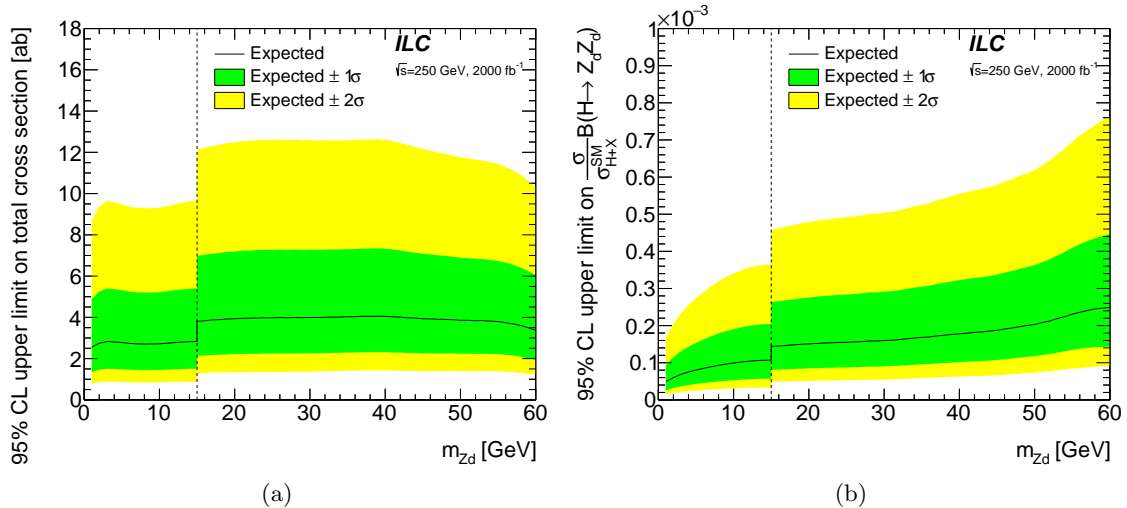
Figure 5: (a) Expected upper limit at 95% CL for the cross section of the $e^+e^- \to H+X \to Z_\mathrm{d}Z_\mathrm{d} + X \to 4\ell + X$ process, assuming SM Higgs boson production. (b) Expected upper limit at 95% CL for the cross section times the model-dependent branching ratio divided by the SM Higgs boson production cross section (319 fb) for the $H \to Z_\mathrm{d}Z_\mathrm{d}$ process for the benchmark HAHM. In both cases, all final states are combined. The discontinuities at $m_{Z_\mathrm{d}} = 15\,\mathrm{GeV}$ are due to the change from the LM to HM selection.

or photons. If there are multiple eligible lepton pairs, the one with invariant mass closest to the Z-boson mass m_Z is selected as the Z or Z_d candidate. The $4j$ final state has no requirement on the number of isolated leptons, but requires six jets from non-isolated PFO objects. Either case uses the standard jet reconstruction to four or six jets, respectively.

For both final states, all possible jet pairs are constructed. The invariant masses of the jet pairs, along with the dilepton's invariant mass in the $2\ell2j$ final state, are compared against m_Z and the pair with the invariant mass closest to m_Z is selected as the Z-boson candidate. If in the $2\ell2j$ final state preselection a jet pair is selected as the Z-candidate, the remaining jet and lepton pairs are selected as the Z_d candidates. In all other cases all possible jet pairs from the remaining four jets are constructed and the two jet pairs with invariant mass closest to each other, i.e. minimizing $|m_{j_1j_2} - m_{j_3j_4}|$, are selected as the two Z_d candidates.

The jets, as well as leptons in the $2\ell2j$ case, must satisfy the requirement on their polar angle $|\cos(\theta)| < 0.9$.

The final requirement for the preselection is that the four fermions constituting the two Z_d candidates have a total invariant mass broadly consistent with that of the Higgs boson: $90\,\mathrm{GeV} < m_{ffff} < 160\,\mathrm{GeV}$.

The preselection efficiency $\times$ acceptance for the signal samples is around 31% for the $4j$ final state and 24% for the $2\ell2j$ one. For the background samples the efficiencies $\times$

Table 5: Selection efficiencies $\times$ acceptance for the $4j$ and $2\ell2j$ signal regions after preselection and boosted decision tree selection.

	signal efficiency $\times$ acceptance			background efficiency $\times$ acceptance
m_{Z_d}	20 GeV	40 GeV	60 GeV	
$4j$ final state	9.4%	5.2%	4.7 %	0.02%
$2\ell2j$ final state	24%	22%	24%	0.6%

Table 6: Expected signal region event yields for the $2\ell2j$ and $4j$ final states. Both are scaled to an integrated luminosity of $2000\,\mathrm{fb}^{-1}$. The signal yields assume a $H \to Z_\mathrm{d}Z_\mathrm{d} \to 2\ell2j$, $4j$ cross section of 1 fb.

	signal yields			background yield
m_{Z_d}	20 GeV	40 GeV	60 GeV	
$4j$ final state	187	103	93	8400
$2\ell2j$ final state	484	448	487	131

acceptances are 17% and 2% for the $4j$ and $2\ell2j$ final states, respectively.

The signal regions are defined by boosted decision trees individually trained for each final state. Half of the generated events for both the background and signal samples are randomly assigned for training, while the remainder are used for evaluation. The input variables for the BDT are:

- The transverse momentum, total energy, invariant mass, and $\cos(\theta)$ for each Z-boson and Z_d-boson candidate;

- the ΔR between each possible boson candidate pair;

- and the transverse momentum, total energy, invariant mass of the Higgs boson candidate.

The efficiencies after the preselection and the BDT selection for the signals and background are shown in Table 5, and Table 6 shows the signal region event yields assuming an integrated luminosity of $2000\,\mathrm{fb}^{-1}$ and an $H \to Z_\mathrm{d}Z_\mathrm{d} \to 2\ell2j$, $4j$ cross section of 1 fb.

7 $H \to Z_\mathbf{d}Z_\mathbf{d} \to 2\ell2j$, $4j$ expected limits

The likelihood function describing the data for the $4j$ and $2\ell2j$ final states follows Eq. (1). Both final state channels are fitted concurrently so the model in this case is given by:

$$\mathcal{L}(N) = \prod_{j=4j,2l2j} \prod_i \mathrm{Pois}\left(N_{ij}; \mu S_{ij}(m_{Z_\mathrm{d}}) + B_{ij}\right). \tag{2}$$
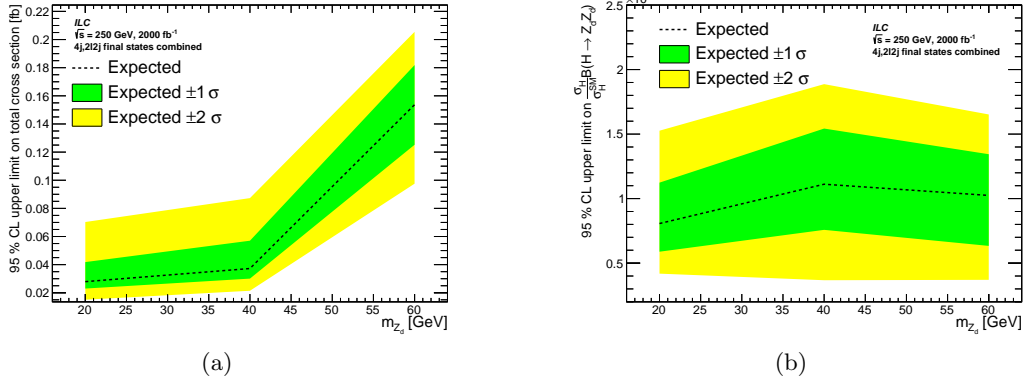
Figure 6: (a) Expected upper limit at 95% CL for the cross section of the $e^+e^- \to H + Z \to Z_{\rm d}Z_{\rm d} + Z \to 4j, 2\ell 2j + Z$ process, assuming SM Higgs boson production. (b) Expected upper limit at 95% CL on the $H \to Z_{\rm d}Z_{\rm d}$ branching ratio, derived from the $e^+e^- \to H + Z \to Z_{\rm d}Z_{\rm d} + Z \to 4j, 2\ell 2j + Z$ cross section.

The distributions used to evaluate the likelihood are the average $Z_{\rm d}$ mass: $\langle m_{Z_d} \rangle = \frac{1}{2}(m_{Z_{\rm d1}} + m_{Z_{\rm d2}})$. The limits on the total cross section for the combined $4j$ and $2\ell 2j$ branching ratio are shown in Fig. 6a.

Fig. 6b shows that the $2\ell 2j$ and $4j$ final states do not yield a stricter expected limit on $\mathrm{BR}(H \to Z_{\rm d}Z_{\rm d})$ than the 4ℓ final state, despite the more favorable $\mathrm{BR}(Z_{\rm d} \to 2j)$ branching ratio [6].

8 Summary and future work

Expected limits have been presented for a search for dark photons in the $H \to Z_{\rm d}Z_{\rm d} \to 4\ell$, $2\ell 2j$, and $4j$ final states. It is seen that compared to the LHC, searches for these channels are not competitive at the ILC, except for $Z_{\rm d}$ masses close to the J/ψ and Υ quarkonia resonances. The LHC analysis does not have sensitivity in those region due to large hadronic backgrounds, but it should be possible to derive limits in those regions at the ILC where such backgrounds are much smaller. Doing this reliably, however, will likely require progress in theoretical calculations of decays involving quarkonia states.

Acknowledgments

References

[1] P. Fayet, "Light spin-1/2 or spin-0 dark matter particles", *Phys. Rev. D* 70 (2004), p. 023514, DOI: 10.1103/PhysRevD.70.023514, arXiv: hep-ph/0403226 [hep-ph].

[2] D. P. Finkbeiner and N. Weiner, "Exciting dark matter and the INTEGRAL/SPI 511 keV signal", *Phys. Rev. D* 76 (2007), p. 083519, DOI: 10.1103/PhysRevD.76.083519, arXiv: astro-ph/0702587 [astro-ph].

[3] N. Arkani-Hamed et al., "A theory of dark matter", *Phys. Rev. D* 79 (2009), p. 015014, DOI: 10.1103/PhysRevD.79.015014, arXiv: 0810.0713 [hep-ph].

[4] E. Dudas et al., "Extra U(1) as natural source of a monochromatic gamma ray line", *JHEP* 10 (2012), p. 123, DOI: 10.1007/JHEP10(2012)123, arXiv: 1205.1520 [hep-ph].

[5] D. Curtin et al., "Illuminating dark photons with high-energy colliders", *JHEP* 02 (2015), p. 157, DOI: 10.1007/JHEP02(2015)157, arXiv: 1412.0018 [hep-ph].

[6] D. Curtin et al., "Exotic decays of the 125 GeV Higgs boson", *Phys. Rev. D* 90.7 (2014), p. 075004, DOI: 10.1103/PhysRevD.90.075004, arXiv: 1312.4992 [hep-ph].

[7] H. Davoudiasl et al., "Higgs decays as a window into the dark sector", *Phys. Rev. D* 88.1 (2013), p. 015022, DOI: 10.1103/PhysRevD.88.015022, arXiv: 1304.4935 [hep-ph].

[8] H. Davoudiasl, H.-S. Lee, and W. J. Marciano, ""Dark" Z implications for parity violation, rare meson decays, and Higgs physics", *Phys. Rev. D* 85 (2012), p. 115019, DOI: 10.1103/PhysRevD.85.115019, arXiv: 1203.2947 [hep-ph].

[9] J. D. Wells, "How to Find a Hidden World at the Large Hadron Collider" (2008), arXiv: 0803.1243 [hep-ph].

[10] S. Gopalakrishna, S. Jung, and J. D. Wells, "Higgs boson decays to four fermions through an abelian hidden sector", *Phys. Rev. D* 78 (2008), p. 055002, DOI: 10.1103/PhysRevD.78.055002, arXiv: 0801.3456 [hep-ph].

[11] J. Alexander et al., *Dark Sectors 2016 Workshop: Community Report*, 2016, arXiv: 1608.08632 [hep-ph].

[12] P. Galison and A. Manohar, "Two Z's or not two Z's?", *Phys. Lett. B* 136 (1984), p. 279, DOI: 10.1016/0370-2693(84)91161-4.

[13] B. Holdom, "Two U(1)'s and ϵ charge shifts", *Phys. Lett. B* 166 (1986), p. 196, DOI: 10.1016/0370-2693(86)91377-8.

[14] K. R. Dienes, C. F. Kolda, and J. March-Russell, "Kinetic mixing and the supersymmetric gauge hierarchy", *Nucl. Phys. B* 492 (1997), pp. 104–118, DOI: 10.1016/S0550-3213(97)00173-9, arXiv: hep-ph/9610479 [hep-ph].

[15] ATLAS Collaboration, "Search for Higgs bosons decaying into new spin-0 or spin-1 particles in four-lepton final states with the ATLAS detector with $139\,\mathrm{fb}^{-1}$ of pp collision data at $\sqrt{s} = 13\,\mathrm{TeV}$" (2021), arXiv: 2110.13673 [hep-ex].

[16]   ATLAS Collaboration, "Search for Higgs boson decays into two new low-mass spin-0 particles in the $4b$ channel with the ATLAS detector using pp collisions at $\sqrt{s} = 13\,\mathrm{TeV}$", *Phys. Rev. D* 102 (2020), p. 112006, DOI: 10.1103/PhysRevD.102.112006, arXiv: 2005.12236 [hep-ex].

[17]   ATLAS Collaboration, "Search for Higgs boson decays into pairs of light (pseudo)scalar particles in the $\gamma\gamma jj$ final state in pp collisions at $\sqrt{s} = 13\,\mathrm{TeV}$ with the ATLAS detector", *Phys. Lett. B* 782 (2018), p. 750, DOI: 10.1016/j.physletb.2018.06.011, arXiv: 1803.11145 [hep-ex].

[18]   ATLAS Collaboration, "Search for the Higgs boson produced in association with a vector boson and decaying into two spin-zero particles in the $H \to aa \to 4b$ channel in pp collisions at $\sqrt{s} = 13\,\mathrm{TeV}$ with the ATLAS detector", *JHEP* 10 (2018), p. 031, DOI: 10.1007/JHEP10(2018)031, arXiv: 1806.07355 [hep-ex].

[19]   ATLAS Collaboration, "Search for Higgs boson decays into a pair of light bosons in the $bb\mu\mu$ final state in pp collision at $\sqrt{s} = 13\,\mathrm{TeV}$ with the ATLAS detector", *Phys. Lett. B* 790 (2019), p. 1, DOI: 10.1016/j.physletb.2018.10.073, arXiv: 1807.00539 [hep-ex].

[20]   ATLAS Collaboration, "Search for Higgs bosons decaying to aa in the $\mu\mu\tau\tau$ final state in pp collisions at $\sqrt{s} = 8\,\mathrm{TeV}$ with the ATLAS experiment", *Phys. Rev. D* 92 (2015), p. 052002, DOI: 10.1103/PhysRevD.92.052002, arXiv: 1505.01609 [hep-ex].

[21]   CMS Collaboration, "A search for pair production of new light bosons decaying into muons", *Phys. Lett. B* 752 (2016), p. 146, DOI: 10.1016/j.physletb.2015.10.067, arXiv: 1506.00424 [hep-ex].

[22]   CMS Collaboration, "Search for light bosons in decays of the $125\,\mathrm{GeV}$ Higgs boson in proton–proton collisions at $\sqrt{s} = 8\,\mathrm{TeV}$", *JHEP* 10 (2017), p. 076, DOI: 10.1007/JHEP10(2017)076, arXiv: 1701.02032 [hep-ex].

[23]   CMS Collaboration, "Search for a light pseudoscalar Higgs boson in the boosted $\mu\mu\tau\tau$ final state in proton–proton collisions at $\sqrt{s} = 13\,\mathrm{TeV}$", *JHEP* 08 (2020), p. 139, DOI: 10.1007/JHEP08(2020)139, arXiv: 2005.08694 [hep-ex].

[24]   CMS Collaboration, "Search for long-lived particles decaying into muon pairs in proton–proton collisions at $\sqrt{s} = 13\,\mathrm{TeV}$ collected with dedicated high-rate data stream" (2021), arXiv: 2112.13769 [hep-ex].

[25]   LHCb Collaboration, "Search for Dark Photons Produced in 13 TeV pp Collisions", *Phys. Rev. Lett.* 120.6 (2018), p. 061801, DOI: 10.1103/PhysRevLett.120.061801, arXiv: 1710.02867 [hep-ex].

[26]   ATLAS Collaboration, "Search for long-lived neutral particles decaying into lepton jets in proton–proton collisions at $\sqrt{s} = 8\,\mathrm{TeV}$ with the ATLAS detector", *JHEP* 11 (2014), p. 088, DOI: 10.1007/JHEP11(2014)088, arXiv: 1409.0746 [hep-ex].

[27]   ATLAS Collaboration, "A search for prompt lepton-jets in pp collisions at $\sqrt{s} = 8\,\mathrm{TeV}$ with the ATLAS detector", *JHEP* 02 (2016), p. 062, DOI: 10.1007/JHEP02(2016)062, arXiv: 1511.05542 [hep-ex].

[28]   ATLAS Collaboration, "Search for massive, long-lived particles using multitrack displaced vertices or displaced lepton pairs in pp collisions at $\sqrt{s} = 8\,\mathrm{TeV}$ with the ATLAS detector", *Phys. Rev. D* 92 (2015), p. 072004, DOI: 10.1103/PhysRevD.92.072004, arXiv: 1504.05162 [hep-ex].

[29]   CMS Collaboration, "Search for long-lived particles that decay into final states containing two electrons or two muons in proton–proton collisions at $\sqrt{s} = 8\,\mathrm{TeV}$", *Phys. Rev. D* 91 (2015), p. 052012, DOI: 10.1103/PhysRevD.91.052012, arXiv: 1411.6977 [hep-ex].

[30]   ATLAS Collaboration, "Search for long-lived particles in final states with displaced dimuon vertices in pp collisions at $\sqrt{s} = 13\,\mathrm{TeV}$ with the ATLAS detector", *Phys. Rev. D* 99 (2019), p. 012001, DOI: 10.1103/PhysRevD.99.012001, arXiv: 1808.03057 [hep-ex].

[31]   ATLAS Collaboration, "Search for displaced vertices of oppositely charged leptons from decays of long-lived particles in pp collisions at $\sqrt{s} = 13\,\mathrm{TeV}$ with the ATLAS detector", *Phys. Lett. B* 801 (2020), p. 135114, DOI: 10.1016/j.physletb.2019.135114, arXiv: 1907.10037 [hep-ex].

[32]   ATLAS Collaboration, "Search for light long-lived neutral particles produced in pp collisions at $\sqrt{s} = 13\,\mathrm{TeV}$ and decaying into collimated leptons or light hadrons with the ATLAS detector", *Eur. Phys. J. C* 80 (2020), p. 450, DOI: 10.1140/epjc/s10052-020-7997-4, arXiv: 1909.01246 [hep-ex].

[33]   ATLAS Collaboration, "Constraints on mediator-based dark matter and scalar dark energy models using $\sqrt{s} = 13\,\mathrm{TeV}$ pp collision data collected by the ATLAS detector", *JHEP* 05 (2019), p. 142, DOI: 10.1007/JHEP05(2019)142, arXiv: 1903.01400 [hep-ex].

[34]   CMS Collaboration, "A search for pair production of new light bosons decaying into muons in proton–proton collisions at $13\,\mathrm{TeV}$", *Phys. Lett. B* 796 (2019), p. 131, DOI: 10.1016/j.physletb.2019.07.013, arXiv: 1812.00380 [hep-ex].

[35]   ATLAS Collaboration, "Combination of Searches for Invisible Higgs Boson Decays with the ATLAS Experiment", *Phys. Rev. Lett.* 122 (2019), p. 231801, DOI: 10.1103/PhysRevLett.122.231801, arXiv: 1904.05105 [hep-ex].

[36]   CMS Collaboration, "Search for invisible decays of a Higgs boson produced through vector boson fusion in proton–proton collisions at $\sqrt{s} = 13\,\mathrm{TeV}$", *Phys. Lett. B* 793 (2019), p. 520, DOI: 10.1016/j.physletb.2019.04.025, arXiv: 1809.05937 [hep-ex].

[37]   J. Alwall et al., "The automated computation of tree-level and next-to-leading order differential cross sections, and their matching to parton shower simulations", *JHEP* 07 (2014), p. 079, DOI: 10.1007/JHEP07(2014)079, arXiv: 1405.0301 [hep-ph].

[38]   T. Sjöstrand et al., "An introduction to PYTHIA 8.2", *Comput. Phys. Commun.* 191 (2015), p. 159, DOI: 10.1016/j.cpc.2015.01.024, arXiv: 1410.3012 [hep-ph].

[39]   W. Kilian, T. Ohl, and J. Reuter, "WHIZARD: Simulating Multi-Particle Processes at LHC and ILC", *Eur. Phys. J. C* 71 (2011), p. 1742, DOI: 10.1140/epjc/s10052-011-1742-y, arXiv: 0708.4233 [hep-ph].

[40] M. Moretti, T. Ohl, and J. Reuter, "O'Mega: An Optimizing matrix element generator" (Feb. 2001), ed. by T. Behnke et al., pp. 1981–2009, arXiv: hep-ph/0102195.

[41] T. Sjöstrand, S. Mrenna, and P. Z. Skands, "PYTHIA 6.4 physics and manual", *JHEP* 05 (2006), p. 026, DOI: 10.1088/1126-6708/2006/05/026, arXiv: hep-ph/0603175.

[42] D. Jeans and C. Potter, *Snowmass Energy Frontier ILC Analysis Walkthrough*, Talk given at the Oct. 2020 Snowmass tutorial, URL: https://indico.fnal.gov/event/45721/contributions/198054/attachments/136223/169374/snowmass-walkthrough-v3.pdf.

[43] iLCSoft authors, *iLCSoft Project Page*, URL: https://github.com/iLCSoft.

[44] H. Abramowicz et al., "The International Linear Collider Technical Design Report - Volume 4: Detectors" (June 2013), ed. by T. Behnke et al., arXiv: 1306.6329 [physics.ins-det].

[45] C. Duerig and J. Tian, *A new MVA based Isolated Lepton Tagging Processor*, URL: https://github.com/iLCSoft/MarlinReco/tree/master/Analysis/IsolatedLeptonTagging.

[46] C. Potter, "SiD Simulation & Analysis for ILC Snowmass Physics LoIs", *arXiv preprint arXiv:2106.00819* (2021).

[47] P. Zyla et al., "Review of Particle Physics", *Prog. Theor. Exp. Phys.* 2020 (2020), p. 083C01, DOI: 10.1093/ptep/ptaa104.

[48] H.-S. Shao, "HELAC-Onia 2.0: an upgraded matrix-element and event generator for heavy quarkonium physics", *Comput. Phys. Commun.* 198 (2016), pp. 238–259, DOI: 10.1016/j.cpc.2015.09.011, arXiv: 1507.03435 [hep-ph].

[49] H.-S. Shao, "HELAC-Onia: An automatic matrix element generator for heavy quarkonium physics", *Comput. Phys. Commun.* 184 (2013), pp. 2562–2570, DOI: 10.1016/j.cpc.2013.05.023, arXiv: 1212.5293 [hep-ph].

[50] D.-N. Gao and X. Gong, "Higgs boson decays into a pair of heavy vector quarkonia" (Mar. 2022), arXiv: 2203.00514 [hep-ph].

[51] V. Kartvelishvili, A. V. Luchinsky, and A. A. Novoselov, "Double vector quarkonia production in exclusive Higgs boson decays", *Phys. Rev. D* 79 (2009), p. 114015, DOI: 10.1103/PhysRevD.79.114015, arXiv: 0810.0953 [hep-ph].

[52] W. Verkerke and D. Kirkby, *The RooFit toolkit for data modeling*, 2003, arXiv: physics/0306116 [physics.data-an].

[53] K. S. Cranmer, "Kernel estimation in high-energy physics", *Comput. Phys. Commun.* 136 (2001), pp. 198–207, DOI: 10.1016/S0010-4655(00)00243-5, arXiv: hep-ex/0011057 [hep-ex].

[54] ATLAS Collaboration, *Proposal for particle-level object and observable definitions for use in physics measurements at the LHC*, ATL-PHYS-PUB-2015-013, 2015, URL: https://cds.cern.ch/record/2022743.

[55] A. L. Read, "Presentation of search results: the CL_S technique", *J. Phys. G* 28 (2002), p. 2693, DOI: 10.1088/0954-3899/28/10/313.

[56] G. Cowan et al., "Asymptotic formulae for likelihood-based tests of new physics",
      Eur. Phys. J. C 71 (2011), p. 1554, DOI: 10.1140/epjc/s10052-011-1554-0, arXiv:
      1007.1727 [physics.data-an], Erratum: Eur. Phys. J. C **73** (2013) 2501.